

# The role of tin and magnesium in assisting liquid phase sintering of aluminum (Al)

Nur Ayuni Jamal<sup>1</sup>, Farazila Yusof<sup>2</sup>, Yusilawati Ahmad Nor<sup>3</sup>, Maizatunlisa Othman<sup>1</sup>, Khalisanni Khalid<sup>4</sup> and Muhamad Nazarudin Zakaria<sup>5</sup>

<sup>1</sup>Manufacturing and Materials Engineering (MME) Department, Kuliyah of Engineering, International Islamic University Malaysia, P.O. Box 10, 50728, Kuala Lumpur, Malaysia

<sup>2</sup>Centre of Advanced Manufacturing and Materials Processing (AMMP), Faculty of Engineering, University Malaya, 50603, Kuala Lumpur, Malaysia

<sup>3</sup>Biotechnology Engineering Department, Kuliyah of Engineering, International Islamic University Malaysia, P.O. Box 10, 50728, Kuala Lumpur, Malaysia

<sup>4</sup>Food and Agriculture Analysis Laboratory Program, Technical Service Centre, Malaysian Agricultural Research and Development Institute (MARDI), 43400 Serdang, Selangor, Malaysia

<sup>5</sup>Bio-composite Technology Programme, School of Industrial Technology, Faculty of Applied Sciences, University Technology MARA, 40450, Shah Alam, Selangor, Malaysia of Manufacturing and Materials Engineering, International Islamic University Malaysia (IIUM), Jalan Gombak, 53100 Kuala Lumpur, Malaysia

Email: ayuni\_jamal@iium.edu.my

**Abstract.** This study aims to investigate the effect of tin (Sn) and magnesium (Mg) on the sintering response of sintered Al. Although this topic has been extensively reported, details on the combined effect of Sn and Mg that function as sintering additives are still limited. The current study discusses the effect of the combined use of Sn and Mg to assist aluminium (Al) in liquid phase sintering via the powder metallurgy technique. The results demonstrated that the densities of sintered Al increased from 2.5397 to 2.575 g/cm<sup>3</sup> as the Sn content increased from 1.5 to 2.5 wt. % respectively. Accordingly, the physical characteristics of sintered Al were transformed from black to silver, which confirmed the reduction in the oxygen content (oxide layer reduction) from 0.58 to 0.44 wt. % respectively. Additionally, the microstructure of the resultant sintered Al demonstrated that effective wetting by Sn addition was obtained at its maximum content of 2.5 wt. % with a greater micro pores reduction and better metallurgical bonding between Al particles. Therefore, the introduction of different Sn content, along with Mg element, was found to further improve the sintering response of the resultant sintered Al that consequently improved its densities and physical characteristics.

## 1. Introduction

Aluminium (Al) and its alloys have been extensively exploited in the automotive and aerospace industries due several prominent properties including low density, low melting temperature, high corrosion resistance and excellent electrical and thermal properties [1, 2]. Various processing

techniques, including casting and powder metallurgy, have been generally utilized to fabricate Al and its alloys [3, 4]. Owing to the efficient materials utilization, greater control of starting materials ratio, and capability to produce complex products with uniform microstructure, the latter process has been widely applied in fabricating Al and its alloys [3-5]. In a recent study by Mahesh et al. [4], titanium nitride (TiN) reinforced Al composites with a maximum compressive strength of 150 MPa have been successfully fabricated using the powder metallurgy technique. However, the processing of Al and its alloys is considered a challenging task, attributable to the existence of thermodynamically stable layers (1-2 nm thickness) of aluminium oxide ( $\text{Al}_2\text{O}_3$ ) on the powder surfaces [6, 7]. As such, effective metallurgical bonding among Al particles cannot be obtained during sintering, since they hinder the enhancement of the physical and mechanical properties of the resultant Al and its alloys. Liquid phase sintering by means of sintering additives addition has been commonly introduced to overcome the abovementioned problem [6-8]. Magnesium (Mg) and tin (Sn) elements are broadly employed as sintering additives in order to assist Al in liquid phase sintering [6-8]. MacAskill et al. [8] and Sercombe et al. [6] have been reported that the utilization of sintering additives (Mg and Sn) enhanced the sintering response of sintered Al, which consequently improved its tensile strength up to 118 MPa and 300 MPa respectively.

Despite progressive work on the sintering response of Al and its alloys via the powder metallurgy technique, further investigation is required, especially with different formulations of Al and sintering additives. Therefore, the current study focused on the use of Mg and Sn elements as sintering additives in assisting liquid phase sintering of Al via the powder metallurgy method. More specifically, the effects of various Sn content and fixed Mg content on the physical characteristics, oxygen content levels, density and microstructure of sintered Al were examined. The present work will provide additional knowledge on the existing behaviour of liquid phase sintering of Al and its alloys.

## **2. Materials and Methods**

### *2.1 Raw materials*

Elemental Al powder (99.9% purity, NovaScientific, Malaysia), with an average particle size of 45  $\mu\text{m}$ , was used as the matrix constituent, whereas elemental Mg (99.9% purity, NovaScientific, Malaysia) and Sn powders (99.5% purity, Sigma Aldrich, Malaysia) with average particle sizes of 10 and 45  $\mu\text{m}$  were introduced as sintering additives to initiate the liquid phase sintering of Al. In this study, the content of Mg was fixed at 0.5 wt. %, while the Sn content varied between 1.5, 2 and 2.5 wt. % respectively.

### *2.2 Preparation of sintered Al compact*

The sintered Al compact was prepared using the powder metallurgy method, which comprises mixing, compaction and sintering, as schematically illustrated in figure 1. The elemental powder mixture containing Al, Mg and Sn was initially mixed in a table-top ball mill with the powder-to-ball (Zirconia) ratio of 1:10, for a 12 h period. The elemental mixed powder was then cold compacted in a cylindrical die of 10 mm in diameter and 6 mm in height, at an applied pressure of 250 MPa. Next, the compacted specimen was sintered at 580 °C for 2 h under Argon ambient to obtain the pure sintered Al body. Finally, the sintered Al specimen was washed with acetone and dried in an electrical oven at 90 °C overnight to remove impurities, prior to characterization.

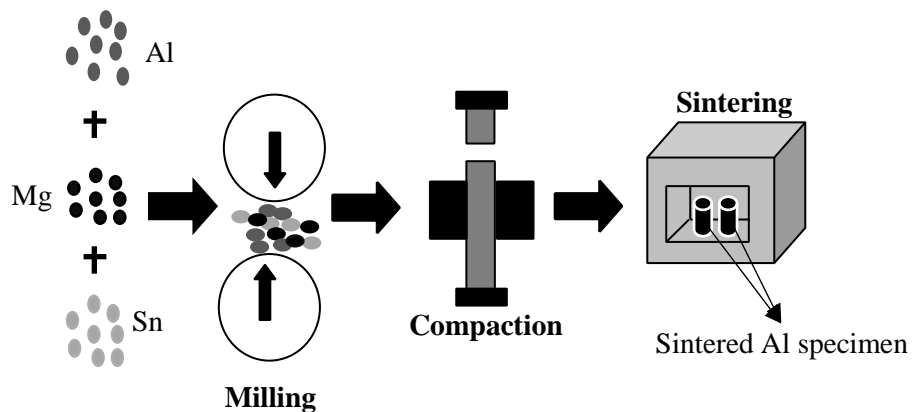


**Figure 1.** Schematic flow diagram of sintered Al preparation.

### 2.3 Characterization techniques

The morphology of the as-received starting powders and the elemental powder mixture were observed using a scanning electron microscope (SEM, Jeol JSM6500F, JEOL Ltd., Tokyo, Japan). In terms of the microscopic examination of the sintered specimen, a cross-section of the specimen was prepared. The microstructure of the cross-section was viewed by SEM. In conjunction with SEM, the distribution of Sn element as well as oxygen content analysis using energy dispersive spectroscopy (EDS) was carried out to identify the remaining content of Sn after sintering and oxygen at every stage. The phase transformation of elemental powder mixture and sintered Al was monitored using X-ray diffraction analysis (XRD; PANalytical X'Pert 1032, Eindhoven, Netherlands) in the  $2\theta$  range of  $20-80^\circ$ . The density of the sintered Al was calculated using the Archimedes principle, as described in ASTM C830-93.

## 3. Results and Discussion

### 3.1 Morphology characterization of starting materials

Figure 2 (a-d) illustrates the SEM images of each starting powder and elemental powder mixture. Al and Mg powders were found to be mostly spherical in shape, with some irregular-shaped Al particles, as seen in figure 2 (a-b). Conversely, Sn powder was predominantly irregular in shape, as shown in figure 2 (c). Since Al is a passive material due to the presence of thermo-chemically stable  $\text{Al}_2\text{O}_3$  film, it is important to interrupt this film to form a strong metallurgical bonding between the Al particles. Hence, in this study, Sn powder was added to increase the fluidity of Al during sintering, while Mg powder was served to enhance the segregation of Sn particles on the Al surface [6-8]. On the other hand, a uniform distribution of elemental powder mixture without any powder agglomeration was observed after a sufficient mixing time of 12 h, and a compaction pressure of 250 MPa, as shown in figure 2 (d). Subsequent to the mixing process, the particles of the elemental powder mixture were found to possess a lamellar structure with a nearly constant powder particle size and shape. Repeated welding, fracturing and re-welding of the powder particles was the reason for such a phenomenon during the mixing stage using the ball milling technique [9].

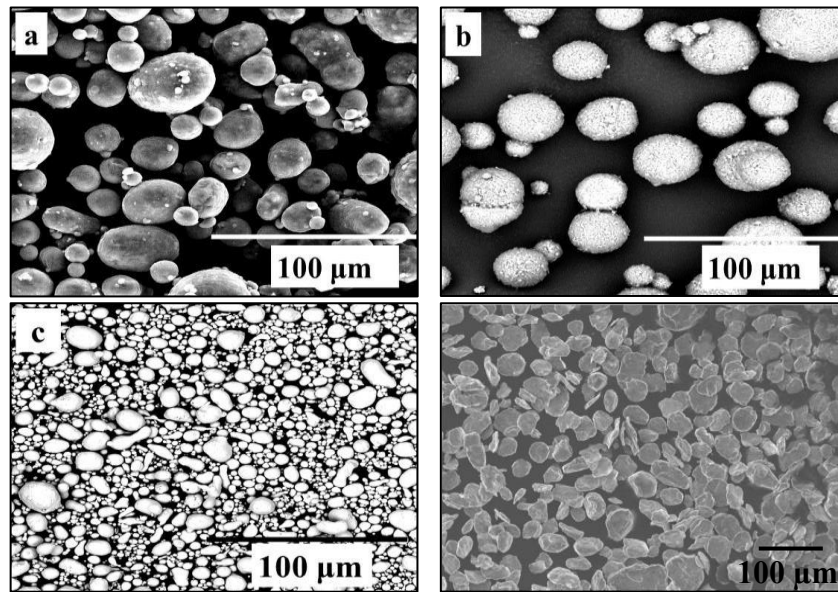


**Figure 2.** SEM micrographs of a) Al powder, b) Mg powder, c) Sn powder and d) Elemental powder mixture after 12 h mixing.

### 3.2 Physical characteristic of sintered aluminum specimen

Figure 3 (a-c) shows the physical characteristics of sintered Al specimen at different Sn content. It can be seen that the black colour of the sintered Al body, which is usually attributed to oxidation (i.e. higher coating of  $\text{Al}_2\text{O}_3$  film on the surface of sintered Al body), was reduced with increasing the Sn content. The highest addition of Sn content (2.5 wt. %) resulted in a silver-like colour that replicated the colour of the starting Al powder. This shows that the film coating of  $\text{Al}_2\text{O}_3$  was greatly disrupted with the addition of a maximum Sn content of 2.5 wt. %. The EDS analysis tabulated in table 1 further confirmed a greater reduction in oxygen content of the resultant sintered Al from 0.58 to 0.44 wt. % with increasing the Sn content from 1.5 to 2.5 wt. % respectively.

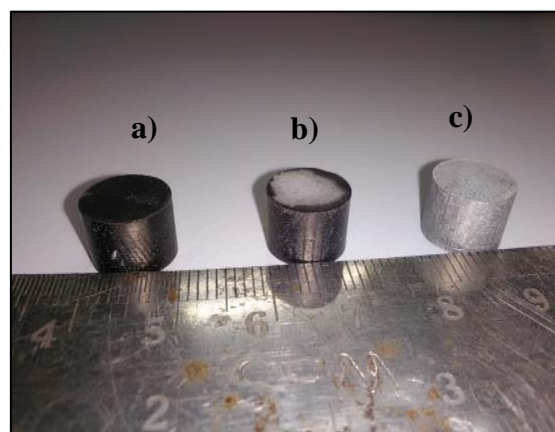


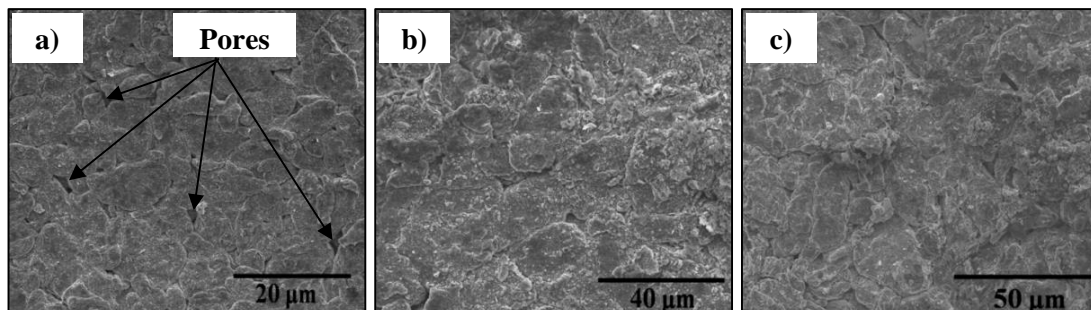
**Figure 3.** Physical characteristic of sintered Al specimen at different Sn content of a) 1.5 wt. %, b) 2 wt. % and c) 2.5 wt. %.

**Table 1.** Oxygen content reading of elemental powder mixture and sintered Al at various Sn content values from EDS analysis. Data are presented in mean  $\pm$  standard deviation.

Tin content (wt. %)	Oxygen Content (wt. %)
Elemental powder mixture	0.22 $\pm$ 0.10
1.5 (sintered at 580 °C)	0.58 $\pm$ 0.12
2 (sintered at 580 °C)	0.51 $\pm$ 0.13
2.5 (sintered at 580 °C)	0.44 $\pm$ 0.11

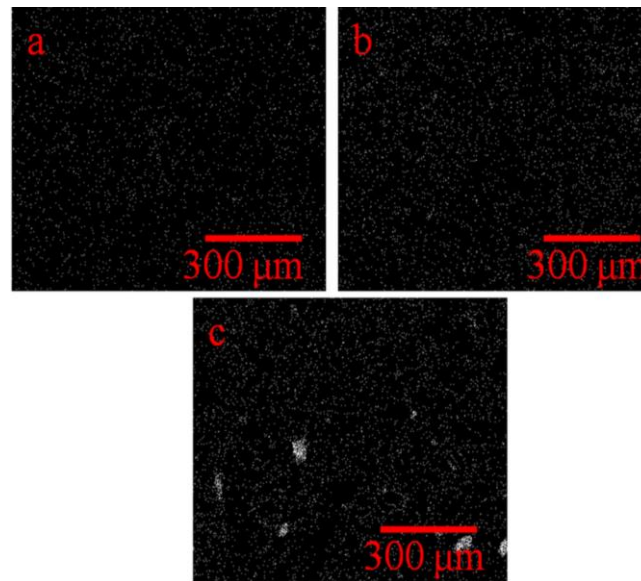
### 3.3 Scanning electron microscopy (SEM) analysis

Figure 4 (a-c) demonstrates the SEM micrographs of the cross section of sintered Al at 1.5, 2 and 2.5 wt. % of Sn content respectively. At low Sn content of 1.5 wt. %, poor sintering quality was observed due to minimal inter-particle necking, profusion of particle boundaries and lack of micro pores rounding (isolated pores), as shown in figure 4 (a). This indicates that the lowest liquid level was found to be inadequate to fill all micro pores, thus preventing efficient metallurgical bonding between Al particles. As such, incomplete elimination of pores could not be obtained due to the insufficient of liquid formation, poor wettability and limited spreading of the liquid phase [10]. Theoretically, Sn melts during sintering and fills the gaps between Al particles and wetting their surfaces [8, 11]. In order to realize this theory, the addition of 0.5 wt. % of Mg was introduced in the current study to break up the  $\text{Al}_2\text{O}_3$  layer and promote metal to metal contact between Al particles prior to liquid phase sintering [8, 11]. On the other hand, the sintering response was found to improve with the addition of 2 and 2.5 wt. % of Sn, as evident in figure 4 (b-c). Furthermore, the presence of particle boundaries also became less noticeable with enhanced inter-particle necking and greater micro pores reduction. It is postulated that a higher liquid level is sufficient to fill the pores due to the effect of Sn wetting on the surface of Al particles that improved the metallic contact among the Al particles [7, 8]. In addition, Sn particles (bright colour) were identified to be homogenously distributed within the microstructure, showing the effective wetting effect of Sn particles on the Al phases that enhanced the densification of sintered Al, as illustrated in figure 5 [8-11]. EDS analysis further confirmed the uniform distribution of Sn element throughout the Al structure as observed in figure 5 (a-c). In relation with this, the number of Sn distribution was found to increase with increasing Sn content. Moreover, this criteria also imply that the associated phase was transformed into liquid during sintering that was able to wet the Al surfaces, and concurrently, spread throughout the compact [8].



**Figure 4.** Microstructure of sintered Al structure at Sn content of a) 1.5 wt. %, b) 2 wt. % and c) 2.5 wt. %.





**Figure 5.** EDS analysis of sintered Al with Sn content of a) 1.5 wt.%, b) 2 wt.% and c) 2.5 wt.%.

### 3.4 X-ray diffraction (XRD) analysis

The XRD patterns of sintered Al with different Sn content values are revealed in figure 6 (a-c). It is worthy to note that the Al rich phase (JCPDS card number 04-0787) was majorly found in the XRD pattern of all of the samples, characterized by the (111), (200), (220) and (311) diffraction peaks at  $38.87^\circ$ ,  $45.42^\circ$ ,  $67.16^\circ$  and  $78.54^\circ$  respectively. No additional peaks were seen in the XRD patterns of all the sintered Al, suggesting the absence of intermetallic phases formation during sintering. On the other hand, the intensity of Sn peak increased with Sn contents, confirming a higher Sn content in the sintered Al. As seen in figure 6 (a-c), the peaks intensities for the sintered Al at Sn content of 2 and 2.5 wt. % were found to be higher as compared to the Sn content of 1.5 wt. %, demonstrating the formation of higher crystalline Al during sintering. However, the presence of Mg peak could hardly be detected, possibly due to the small content of Mg powder employed (0.5 wt.%) during the fabrication process [12].

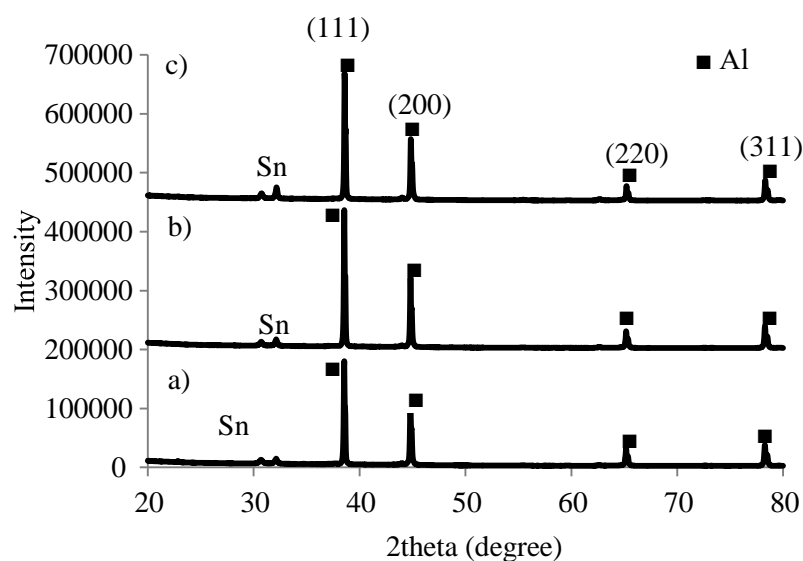


**Figure 6.** XRD patterns of sintered Al with Sn contents of a) 1.5 wt.%, b) 2 wt.% and c) 2.5 wt.%.

### 3.5 Sintered density of aluminum

Figure 7 shows the sintered density of compacted Al at various Sn content values. It can be observed that the sintered density of compacted Al increased as the Sn content increased. The sintered densities of compacted Al increased from 2.5397 to 2.575 g/cm<sup>3</sup> when the Sn content was increased from 1.5 wt. % to 2.5 wt. % respectively. It is clear that the Sn addition promoted the densification of sintered Al. This can be attributed to the pores reduction and particle boundaries disappearance at higher Sn content values, as confirmed by the SEM images in Figure 4 (b-c). In other words, an increased in the sintered density of compacted Al can also be attributed to the fact that higher Sn content produced higher liquid content that can fill all pores with sufficient wettability and spreading of the liquid phase. Su et al. (2013) also reported similar finding in which higher formation of liquid phase was observed to increase the density of the sintered Al due to the porosity reduction. Moreover, considering higher vacancy binding energy and diffusivity of Sn in Al, the vacancies (pores) could be bound with Sn elements, thereby enhanced the sintered density of compacted Al as the liquid phase could persist longer time with increasing Sn content [6-8]. Similarly, Sercombe and Schaffer [6] stated that the formation of liquid phase was slightly slower with the addition of Sn element but larger liquid content could be produced especially greater Sn content that tend to remain for longer time.

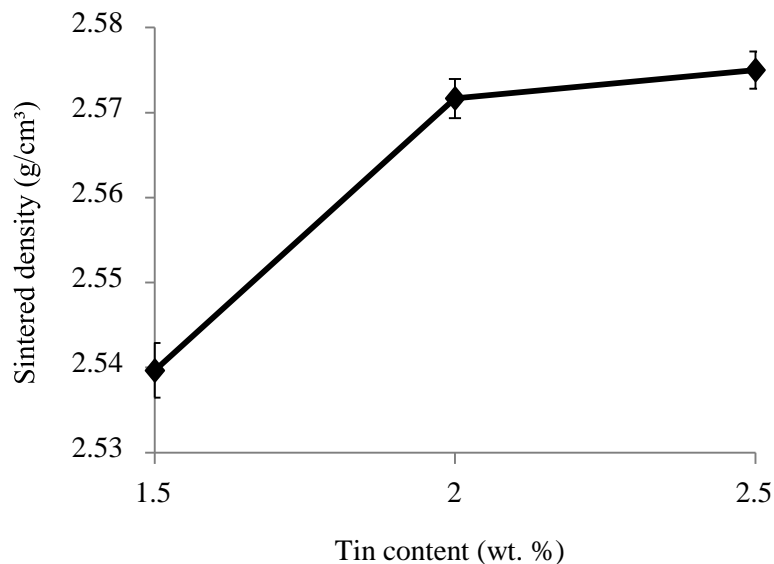


**Figure 7.** Sintered density of compacted Al as a function of different Sn content.

## 4. Conclusion

It can be concluded that the sintering response of the resultant sintered Al highly depends on the combined use of Mg and Sn that serve as sintering additives. In line with this, the physical characteristics (black to silver colour transformation), sintered density (2.575 g/cm<sup>3</sup>) and oxygen content (0.44 wt. %) of the resultant sintered Al improved greatly particularly at a maximum Sn content of 2.5 wt. %. This can be attributed to the effective wetting effect of Sn which was induced by the Mg addition, resulting in micro pores reduction, less formation of particle boundaries and good metallurgical bonding among Al particles, as revealed by the SEM micrographs. The addition of both Mg and Sn have facilitated the sintering response of the resultant sintered Al, which consequently enhanced its densities, physical characteristics and microstructure. Therefore, maximum content of 2.5 wt. % of Sn could be considered as an ideal sintering additive in promoting liquid phase sintering of compacted Al under the current experimental conditions.

### Acknowledgement

The current work was financially supported by a research initiatives grant (RIGS) of International Islamic University Malaysia (IIUM) under project number of 16-091-0255, which is appreciatively acknowledged.

### References

- [1] Aliyu I K, Saheb N, Hassan S F and Al-Aqeeli N 2015 *Metals* **5** 70-83
- [2] Gokce A and Findik F *Scientific Research and Essays* 2011 **6** 4378-4388
- [3] Qiu F, Gao X, Tang J, Gao Y Y, Shu S L, Han X, Li Q and Jiang Q C 2017 *Metals* **7** 3-8
- [4] Mahesh L and Reddy J S 2017 *Mechanics and Mechanical Engineering* **21** 29-36
- [5] Reddy S P, Ramana B and Reddy A C 2010 *International Journal of Materials Science* **5** 777-783
- [6] Sercombe T B and Schaffer G B 1999 *Materials Science and Engineering* **A268** 32– 39
- [7] Katsuyoshi K, Tachai L, Thotsaphon T and Atsushi K 2007 *Transactions of JWRI* **36** 29-33
- [8] MacAskill I A, Hexemer Jr R L, Donaldson I W and Bishop D P 2010 *Journal of Materials Processing Technology* **210** 2252–2260
- [9] Suryanarayana C 2001 *Progress in Materials Science* **46** 1-84
- [10] Su S S, Changa I T H, Kuo W C H 2013 *Materials Chemistry and Physics Journal* **139** 775-782
- [11] Katsuyoshi K, Tachai L, Thotsaphon T and Atsushi K 2007 *Transactions of JWRI* **36** 29-33
- [12] Jha N, Mondala D P, Majumdar J D, Badkul A, Jha A K and Khare A K 2013 *Materials and Design* **47** 810–819